Journal of the Korean Physical Society, Vol. 42, No. 1, January 2003, pp. 162∼166

Self-Organized Patterns in Mixtures of Microtubules and Motor Proteins

Jeenu Kim
School of Physics and Center for Theoretical Physics, Seoul National University, Seoul 151-747 and Supercomputing Research Department, Korea Institute of Science and Technology Information, Daejeon 305-806

Youngah Park*
Department of Physics, Myongji University, Yongin 449-728

Byungnam Kahng
School of Physics and Center for Theoretical Physics, Seoul National University, Seoul 151-747

Ha Youn Lee
Department of Chemical Engineering, University of California, Los Angles, California 90095-1592, U.S.A. and Department of Physics, The Ohio State University, Columbus, Ohio 43210, U.S.A.

(Received 14 August 2002)

We study the self-organized pattern formation occurring in mixtures of microtubules and molecular motors and their density profiles. By separately treating the density profiles of bound and free molecular motors and counting tubule alignments in the motion of bound motors, we develop a continuum equation for the dynamics of motor and microtubule densities. Performing numerical simulations for the dynamic equations with a various motor densities, we find that the mixed pattern of asters and vortices formed at low motor densities gives way to one of vortices alone as the motor density increases. We observe that the density profiles of tubules, free motors, and bound motors can be fitted by logarithmic functions.

PACS numbers: 87.10+e, 87.15-v, 05.10-a
Keywords: Motor protein, Microtubule, Self-organized patterns

I. INTRODUCTION

In eukaryotes, the segregation of replicated chromosomes during cell division occurs on an apparatus called the mitotic spindle [1, 2], which is one of the self-organized patterns emerging in living organisms in nonequilibrium states [3,4]. In the mitotic spindle, microtubules consisting of a subunit called tubulin extend from the two poles of the mitotic spindle to the chromosomes located at the center of the spindle. The slowly growing minus ends of the microtubule orient towards the poles while the fast growing plus ends orient towards chromosomes [5].

Extensive studies of the formation of microtubule asters and mitotic spindles have shown that mechanical forces generated by microtubule-based motor proteins play a crucial role [6,7] in forming the self-organized pattern. Motor proteins are the proteins that are bound to microtubules and walk along them by consuming adenosine triphosphate as a source of energy or are not bound to them. The polarities of the microtubules provide the direction of motion of the motor proteins. For example, kinesin motors move toward microtubule plus ends [8] whereas dynein motors move towards minus ends.

In vitro experiments were carried out [9–11] to understand physical mechanisms involved in the self-organized patterns observed *in vivo* in a system of microtubules and motors. Within a confined cylindrical geometry, microtubules organize into asymmetric asters centered in the chamber at an initial stage, and they continue to grow and begin to buckle. As time goes on, the center of an aster becomes unstable, and a vortex forms in which the motors rotate around the center. A surprising variety of large-scale patterns is formed in a unconfined geometry, depending on the relative concentrations of the molecular components: vortices, asters, and bundles of microtubules emerge with increasing kinesin concentrations.

Some theoretical models have been proposed to describe the dynamics of such patterns observed in those experiments. Simulation results have also been reported [10]. Bassetti *et al.* were successful in producing inhomogeneous stripe patterns by introducing a two-dimensional model for the orientations of micro-

*E-mail: youngah@mju.ac.kr

tubules [12]. Nédélec *et al.* also introduced a convection-diffusion equation for the motor density in the presence of a microtubule array [13] in which the concentration of the microtubule array behaves as $1/r$ with r being the distance from the center of an aster and in which motors detach from and attach to microtubules stochastically. Surrey *et al.* [14] examined how the concentration and kinetic parameters of motor proteins contribute to the self-organized patterns of motor proteins and microtubules. Moreover, Lee and Kardar proposed continuum equations for the evolution of the motor density and for the microtubule orientation. These equations lead to the formation of aster and vortex patterns [15].

Although the dynamics of the microtubule orientation has been considered by Lee and Kardar [15], a continuum dynamics equation which can describe the experimentally observed power-law behavior [13] of the microtubule density has not been considered yet. Also, the stochastic behavior of motor proteins in which motors detach from and attach to the microtubules is known to be important in determining the self-organized pattern of motors and microtubules [14]. In this paper, we develop continuum dynamic equations for microtubules as well as for bound and unbound motors, by extending the continuum equations of Lee and Kardar so that free and bound motor densities are treated separately and the dynamics of the density of microtubules is considered. Through our numerical study of the dynamic equations over a wide range of motor protein densities, we found that the mixed pattern of asters and vortices formed at low motor densities gives way to the one of vortices alone as the motor density increases. We also observe that the density profiles of tubules and free motors around the center of a vortex can be fitted by logarithmic function while that of bound motors can be fitted by the square of a logarithmic function.

II. DYNAMIC EQUATIONS

First, we focus on molecular motors in the presence of tubulin subunits which form microtubules. Molecular motors can exist in two different states, either attached to microtubules or detached from them. Detached (unbound) motors diffuse freely with a diffusion constant D while attached (bound) motors move along their microtubules with a velocity v. We assume that the attachment and the detachment occur stochastically: Bound motors detach spontaneously from microtubules at a rate $p^{\rm off}$, and unbound motors attach to microtubules at a rate $p^{\rm on}$ which has the dimension of a diffusion constant.

We now introduce coarse-grained density functions for bound motors, $b(\boldsymbol{x},t)$, free motors, $f(\boldsymbol{x},t)$, and the tubule field $\boldsymbol{T}(\boldsymbol{x},t)$ to describe the self-organization of microtubules and motors. Bound motors moving along the microtubule with a velocity v creat a bound motor flux

$$\boldsymbol{J}_b = A_b b\hat{T}(\boldsymbol{x},t), \tag{1}$$

where the coefficient A_b is proportional to the velocity v and $\hat{T}$ is the unit vector denoting the direction of the tubule field $\boldsymbol{T}$. Free motors diffuse randomly and create a flux

$$\boldsymbol{J}_f = -D_f \nabla f. \tag{2}$$

We then obtain the coupled dynamic equations for $b(\boldsymbol{x},t)$ and $f(\boldsymbol{x},t)$ [13]:

$$\frac{\partial b}{\partial t} = -p^{\rm off} b + p^{\rm on} T f - \nabla\cdot\boldsymbol{J}_b, \tag{3}$$

$$\frac{\partial f}{\partial t} = p^{\rm off} b - p^{\rm on} T f - \nabla\cdot\boldsymbol{J}_f, \tag{4}$$

where T is the magnitude of the tubule field $\boldsymbol{T}$ describing the density of tubules. While the mixtures of microtubules and motors evolve, the total lengths of microtubules become stabilized. However, the local density of tubules obeys the conservation equation, leading to

$$\frac{\partial T}{\partial t} = -\nabla\cdot\boldsymbol{J}_T, \tag{5}$$

where the tubule current is given as

$$\boldsymbol{J}_T = -D_T\nabla|T| + A_T b\boldsymbol{T}. \tag{6}$$

Here, D_T is the diffusion constant of microtubules, and A_T is the coefficient for describing the tubule motion coupled with bound motors. We assume that A_T is smaller than A_b. For the dynamics of the tubule orientation field $\hat{T}$, we have

$$\frac{\partial \hat{T}}{\partial t} = \nabla\cdot(\gamma b\nabla\hat{T}), \tag{7}$$

which originates from an energy cost of $\frac{1}{2}\gamma b(\nabla T)^2$ for the variation of the tubule orientation. We now rescale the equations into the following dimensionless forms:

$$\frac{\partial f}{\partial t} = p_1 b - p_2 T f + \nabla^2 f \tag{8}$$

$$\frac{\partial b}{\partial t} = -p_1 b + p_2 T f - \nabla\cdot(b\boldsymbol{T}) \tag{9}$$

$$\frac{\partial T}{\partial t} = \frac{D_T}{D_f}\nabla^2 T - \frac{(D_f A_T)}{(\gamma A_b)}\boldsymbol{\nabla}\cdot(b\boldsymbol{T}) \tag{10}$$

$$\frac{\partial \hat{T}}{\partial t} = \boldsymbol{\nabla}\cdot(b\hat{\nabla}\hat{T}), \tag{11}$$

where $p_1 = p^{\rm off}D_f/A_b^2$ and $p_2 = p^{\rm on}\alpha_T D_f/A_b^2$ with α_T being a unit measuring the density of microtubules. Here, we measure length in units of D_f/A_b, time in units of D_f/A_b^2, and motor densities in units of D_f/γ.

III. SIMULATIONS

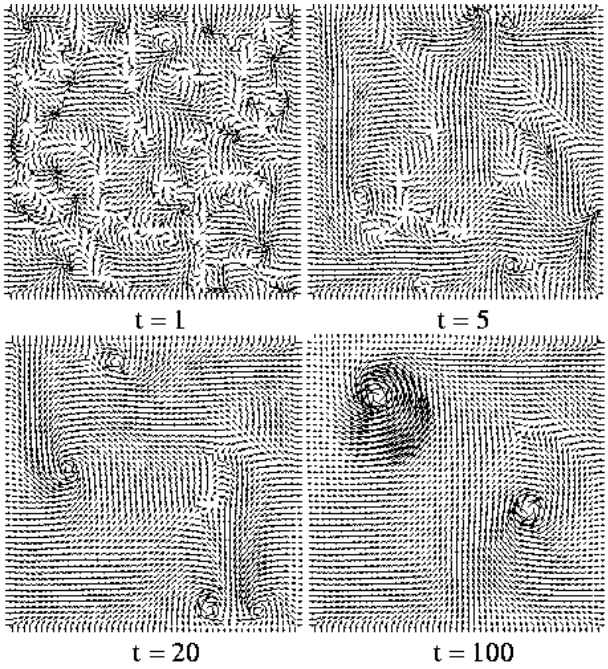

Fig. 1. Self-organized pattern as a function of time for $m_0 = 0.2$.

In performing simulations of the above dynamic equations, we use experimental parameters such as $A_b = 0.8\,\mu$m/s based on the fact that the walking speed of kinesin without a load is $v = 0.8\,\mu$m/s [16, 17]. We also use $p^{\rm off} = 1$/s from direct chemical measurements [18], and $p^{\rm on} = 2.6\,\mu{\rm m}^2$/s and a diffusion constant $D_f = 20\,\mu{\rm m}^2$/s [13]. We set the unit of motor density to be $1/\mu{\rm m}^2$. Since tubules are heavier than motors, we set $A_T D_f/A_b\gamma = 0.1$ and $D_T/D_f = 0.001$.

We now perform numerical simulations on a two-dimensional $L \times L$ lattice by using the Crank-Nicholson scheme with the ADI operator splitting method [19,20]. The equations are discretized with $\Delta x = \Delta y = 0.1$ and a time interval of $\Delta t = 0.0001$. Then the size of the system is 100 μm with $L = 1000$. At the boundary of two dimensional lattice, we employ reflecting boundary conditions where microtubules are pointing inwardly:

$$\hat{T}\big|_{\rm boundary} = -\hat{n} \tag{12}$$

with $\hat{n}$ being the normal outward vector at the boundary.

We start with an initial condition in which the motor density is set to a constant value m_0 for all lattice sites while the magnitude of tubule density field is $T_0 = 1.0$ with random orientation. As time goes on, the homogeneous initial configuration evolves into self-organized patterns, as shown in Fig. 1. The final steady-state pattern depends on the average motor density m_0. Figure 2 shows the self-organized pattern of a mixture of asters and vortices for $m_0 = 0.001$, which is similar to the one obtained by Lee and Kardar [15]. As m_0 is increased further, the sizes of asters and vortices become larger,

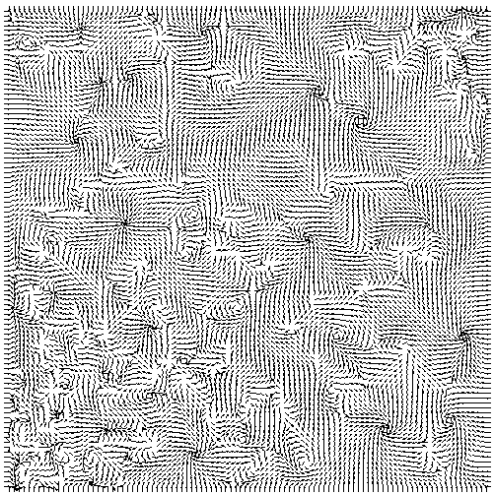

Fig. 2. Mixed pattern of asters and vortices for $m_0 = 0.001$.

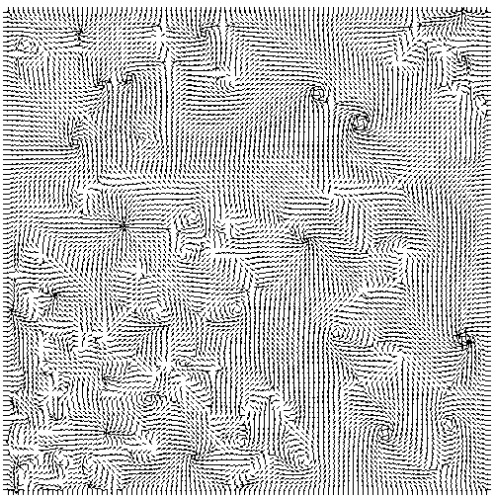

Fig. 3. A mixed pattern of asters and vortices for $m_0 = 0.002$.

and as the average motor density is increased even further, the aster pattern becomes unstable and gives way to a vortex pattern as shown in Figs. 3-5. Finally, a single vortex is observed at $m_0 = 0.2$ [Fig. 6].

We can now find analytic solutions of Eqs. (8)-(11) for the motor densities and the tubule density field. When the pattern is of the vortex form, the direction of the microtubules is described by $\hat{T} = \hat{\theta}$, where $\hat{\theta}$ indicates the tangential unit vector around the center of the vortex. Then, the radial part of the microtubule density can be extracted, and its stationary solution $T(r)$ becomes of the form

$$T(r) \propto -\ln(r/R), \tag{13}$$

where R is a cut-off, corresponding to the mean vortex size. Then, the free motor density function is of a similar form,

$$f \propto -\ln(r/R). \tag{14}$$

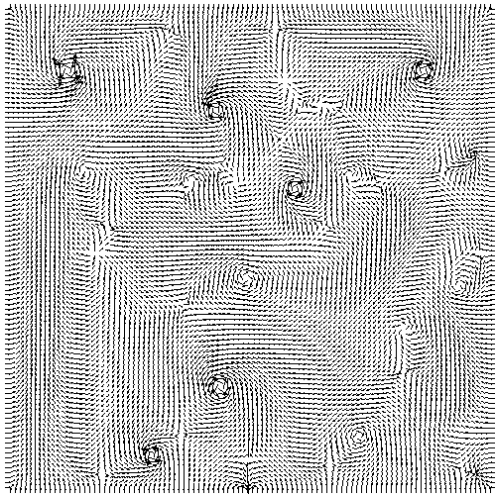

Fig. 4. Mixed pattern of asters and vortices for $m_0 = 0.01$.

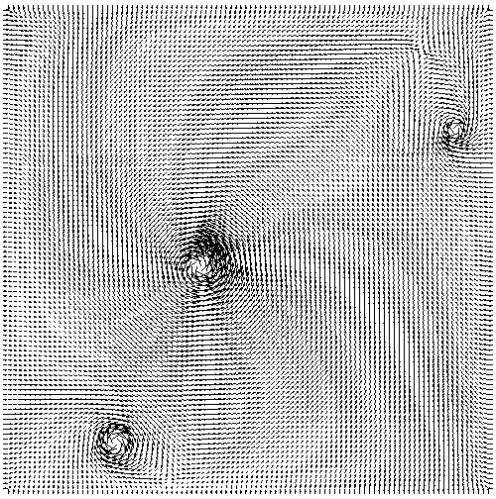

Fig. 5. Pattern of vortices for $m_0 = 0.1$.

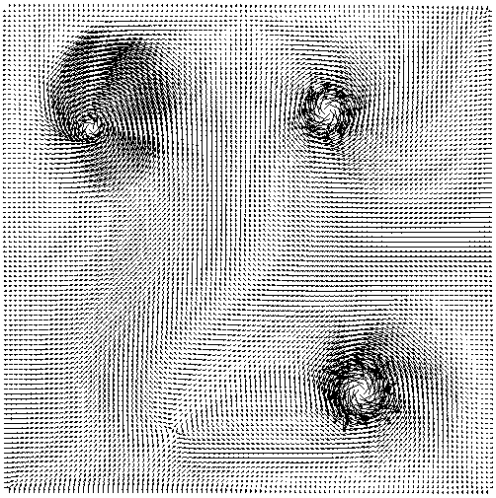

Fig. 6. For $m_0 = 0.2$, a single vortex remains in the self-organized pattern of tubules.

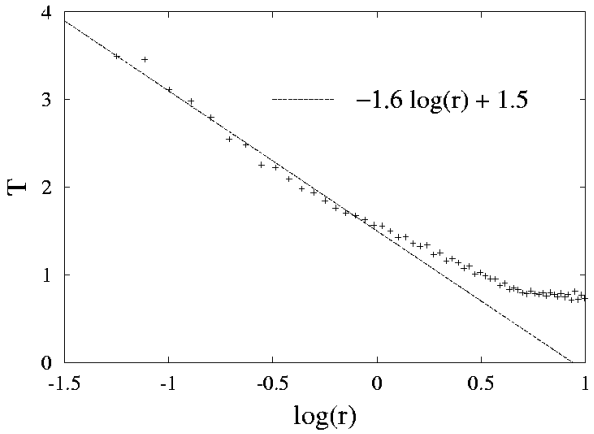

Fig. 7. Profile of the tubule density around the center of a vortex on a semi-log scale for $m_0 = 0.2$ as a function of the distance form the center of a vortex.

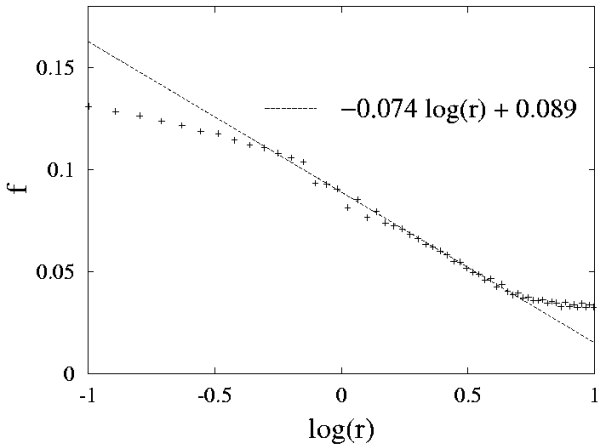

Fig. 8. Profile of the free motor density for $m_0 = 0.2$.

Since the stationary solution for the bound motor density is of the form $(p_1/p_2)T(r)f(r)$ the bound motor density around the vortex is described by

$$b(\boldsymbol{r}) \propto [\ln(r/R)]^2. \tag{15}$$

Figure 7 shows simulated profiles of the tubule density around a vortex for $m_0 = 0.2$ as a function of the distance from the core of the vortex, which can be fitted by a logarithmic function. The densities of bound and free motors are shown in Figs. 8 and 9, respectively, and these can also be fitted by logarithmic-type functions as mentioned above.

In this research, we have studied the self-organized patterns of motor proteins and microtubules by using the continuum dynamics equations for the bound and the free motor densities and the tubule density field. Performing the numerical simulations for various motor densities, we found that a mixed pattern of asters and vortices appears for small motor densities. As the density of motor proteins increases, asters become unstable

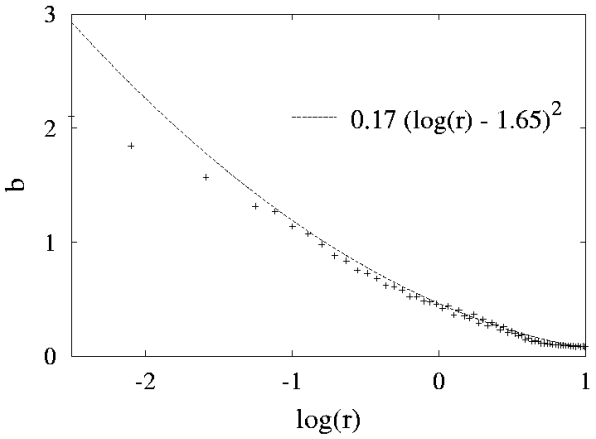

Fig. 9. profile of the bound motor density for $m_0 = 0.2$.

and give way to vortices. We have analyzed the numerical data for the motor densities and the tubule density around the center of a vortex and confirmed that the density profiles are logarithmic-type functions, as predicted by the analytic solutions. It remains to compare our result with experimental data because experimental data of the density for microtubules around an observed lattice of vortices are not yet available [10]. We note that contrary to our results, a lattice of vortices has been obtained at a lower concentration of kinesin motors whereas an irregular lattice of asters has been obtained at a higher concentration in some experiment [10]. This discrepancy originates from geometrical constraints such an aster becoming destabilized by the growth and bucking of microtubules. Vortex patterns were also observed in a solution of tubules and motors in a torus-shaped chamber [10]. This clearly showed the influence of geometrical constraints on self-organization.

In the formation of self-organized patterns of motors and microtubules, it is important that motors have multiple subunits so that the motor complex can bind two microtubules to each other and exert a force on the microtubules. Recently, a numerical work was presented based on a microscopic model that described motor complexes interacting with microtubules [14]. They observed steady-state structures, such as asters and vortices, depending on the kinetic parameters and the motor density They also found that decreasing the residential time of motors (*i.e.*, decreasing the probability that motors will fall off from the ends of microtubules) induced the formation of vortices. Since our model does not yet allow a motor at the end of microtubles to bind two microtubules and exert a force on the tubules, our model might correspond to either the case of a low residential time of motors or low concentration of cross-linking motors. Hence, experimental results similar to ours are expected in such a system.

Although we have not yet developed full coarse-grained equations accounting for the force on the microtubule exerted by cross-linking motors, we have found that the variety of self-organized structures is regulated by various factors such as the motor density, the geometrical factors, and the kinetic parameters. Further work remains to be done in this direction to understand the physical mechanisms of the morphogenetic phenomena taking place in such a biological system.

ACKNOWLEDGMENTS

This work is supported by the Korea Research Foundation grant (KRF 2000-015-DP0103). J.K. was supported by the Korea Science and Engineering Foundation research project No. R01-2000-000-00023-0.

REFERENCES

[1] A. Hyman and E. Karsenti, Cell **84**, 401 (1996).
[2] N. R. Barton and L. S. B. Goldstein, Proc. Natl. Acad. Sci. **93**, 1735 (1996).
[3] M. C. Cross and P. C. Hohenberg, Rev. Mod. Phys. **65**, 851 (1993).
[4] J. P. Gollub and J. S. Langer, Rev. Mod. Phys. **71**, S396 (1999).
[5] For a brief figure of the biological situation, see Ref. 1.
[6] F. Verde, J.-M. Berrez, C. Antony and E. Karsenti, J. Cell Biol. **112**, 1177 (1991).
[7] I. Vorobjev, V. Malikov and V. Rodionov, Proc. Natl. Acad. Sci. USA **98**, 10160 (2001).
[8] A. S. Kashina, R. J. Baskin, D. G. Cole, K. P. Wedaman, W. M. Saxton and J. M. Scholey, Nature **379**, 270 (1996).
[9] R. Urrutia, M. A. McNiven, J. P. Albanesi, D. B. Murphy and B. Kachar, Proc. Natl. Acad. Sci. USA **88**, 6701 (1991)
[10] F. J. Nédélec, T. Surrey, A. C. Maggs and S. Leibler, Nature **389**, 305 (1997).
[11] T. Surrey, M. B. Elowitz, P.-E. Wolf, F. Yang, F. J. Nédélec, K. Shokat and S. Leibler, Proc. Natl. Acad. Sci. USA **95**, 4293 (1998).
[12] B. Bassetti, M. C. Lagomarsino and P. Jona, Eur. Phys. J. B **15**, 483 (2000).
[13] F. J. Nédélec. T. Surrey and A. C. Maggs, Phys. Rev. Lett. **86**, 3192 (2001).
[14] T. Surrey, F. J. Nédélec, S. Leibler and E. Karsenti, Science **292**, 1167 (2001).
[15] H. Y. Lee and M. Kardar, Phys. Rev. E **64**, 056113 (2001).
[16] J. Howard, A. J. Hudspeth and R. D. Vale, Nature **342**, 154 (1989).
[17] K. Svoboda and S. Block, Cell **77**, 773 (1994).
[18] D. Hackney, Nature **377**, 448 (1995).
[19] W. H. Press, S. A. Teukolsky, W. T. Vetterling and B. P. Flannery, *Numerical Recipes in C*, 2nd ed.(Cambridge University Press, Cambridge, 1992).
[20] W. F. Ames, *Numerical Methods for Partial Differential Equation*, 2nd ed. (Academic Press, New York, 1977)